ASSOCIAZIONE NAZIONALE ITALIANA DI INGEGNERIA SISMICA ANIDIS
Italian National Association of Earthquake Engineering

XVIII CONVEGNO ANIDIS
L'ingegneria sismica in Italia
ASCOLI PICENO 2019
15-19 Settembre

Design of hysteretic damped braces for the seismic retrofitting of in-elevation irregularly infilled r.c. framed structures

Fabio Mazza[a], Mirko Mazza[a], Alfonso Vulcano[a]
[a] *Dipartimento di Ingegneria Civile, Università della Calabria, 87036 Rende (CS), Italy*

Keywords: Seismic retrofitting; soft-storey r.c. framed buildings; hysteretic damped braces; displacement-based design; nonlinear dynamic analysis

ABSTRACT
The insertion of steel braces equipped with dampers can be very effective in retrofitting of r.c. framed buildings, provided that suitable layout and properties are selected. A Displacement-Based Design (DBD) procedure, previously proposed for proportioning hysteretic damped braces (HYDBs) in the case of a regular framed building, was extended by the authors in the case of in-elevation irregular layout of masonry infill walls (MIs), whose behaviour was simply assumed as be elastic with brittle failure. To improve reliability and effectiveness of the design procedure, in this paper the hysteretic behaviour of the MIs is taken into account and suitable distributions of the HYDBs properties are proposed aiming to obtain a damped braced structure which can be considered globally regular (e.g., aiming to obtain a same drift ratio and a rather uniform yielding of the hysteretic dampers at all the storeys). A numerical investigation is carried out with reference to a six-storey r.c. framed building, which, primarily designed in compliance with a former Italian seismic code (DM 1996) for a medium-risk zone, is retrofitted by inserting of HYDBs to meet the requirements of the current Italian code (NTC 2018) in a high-risk seismic zone. An in-elevation irregularity of MIs is simulated supposing that, together with a change in use of the building from residential to office, the MIs of the first storey are removed, giving rise to a soft-storey structure. Nonlinear dynamic analyses of the bare frame, soft-storey frame and soft-storey frame retrofitted by HYDBs having different properties are carried out for a set of artificially generated motions whose response spectra match that adopted by NTC 2018 for the life-safety performance level.

1 INTRODUCTION

Masonry infill walls (MIs) can modify significantly the stiffness, strength and mass distributions of a reinforced concrete (r.c.) framed building. Irregularities in the MIs distribution, in elevation (e.g. soft-storeys) or in plan (e.g. unsymmetrical layout), can lead to severe seismic damage [Hak *et al.*, 2012, Braga *et al.*, 2011]. To mitigate these effects and retrofit the structure, damped steel braces with suitable layout and properties can be inserted in the framed structure. Currently a wide variety of energy dissipating devices is available (e.g., see [Soong and Dargush, 1997]). Current seismic codes allow for the use of these devices (e.g. Eurocode 8 [EC8, 2003]; Italian code [NTC18, 2018]) but few codes provide simplified design criteria (e.g. American code [FEMA 356, 2000]).

In a previous work [Mazza and Vulcano, 2014], a Displacement-Based Design (DBD) procedure was proposed for proportioning hysteretic damped braces (HYDBs) in order to retrofit a regular r.c. framed structure, starting from a target deformation of an equivalent elastic linear system with effective properties (see [Priestley *et al.*, 2007]). Then the authors [Mazza *et al.*, 2015] and [Mazza *et al.*, 2017]) extended the DBD procedure in the case of a r.c. framed structure exhibiting in-elevation irregularities of the MIs, whose behaviour was simply assumed to be linear with brittle failure. To overcome this limitation, in this paper design criteria for proportioning the HYDBs are proposed taking into account the hysteretic behaviour of the MIs. Moreover, with reference to a six-storey building with first soft storey, the stiffness distribution of the HYDBs is selected aiming to recover the regularity of the building (e.g., aiming to obtain the same drift ratio at each storey, at least in elastic range, and a rather uniform yielding of the hysteretic dampers at all the storeys).

To check the effectiveness of the proposed design criteria, a numerical investigation is carried out supposing that the r.c. framed building, originally designed according to a former Italian code [DM96, 1996] for a medium-risk zone, has to be retrofitted by inserting of HYDBs to comply with [NTC18, 2018] in a high-risk zone. Nonlinear dynamic responses of the bare frame (BF), irregularly infilled frame (IF) and irregularly-infilled frame retrofitted by HYDBs (IFDB) with different properties, are compared for a set of artificial ground motions compatible with response NTC18 spectrum for the life-safety performance level.

2 DISPLACEMENT-BASED DESIGN OF HYSTERETIC DAMPED BRACES

As mentioned above, a DBD procedure was proposed by [Mazza and Vulcano, 2014] for proportioning the HYDBs in order to attain, for a specific level of seismic intensity, a designated performance level of an existing regular r.c. framed structure. Successively, the DBD procedure was extended to framed buildings with irregular in-elevation distribution of the MIs ([Mazza *et al.*, 2015] and [Mazza *et al.*, 2017]). For this purpose, the response of a single MI was idealized by a diagonal strut model simply assuming an elastic brittle behaviour. The main steps of the design procedure are briefly summarized below with reference to the main assumptions illustrated in Figure 1. More detail can be found in the above papers.

1. Pushover analysis of the unbraced framed building (Figure 1a), which allows to idealize (e.g. as bilinear) the base shear-top displacement ($V^{(F)}$-d) curve and, then, to define an equivalent single degree of freedom (ESDOF) system (Figure 1b) for which the equivalent viscous damping due to hysteresis ($\xi_F^{(h)}$) can be evaluated as depending on the effective ductility level ($\mu_F=d_p/d_y^{(F)}$) and the strain hardening ratio r_F.
2. Evaluation of the equivalent viscous damping due to hysteresis of the damped braces (ξ_{DB}), depending on the effective ductility level ($\mu_{DB}=d_p/d_y^{(DB)}$) and the strain hardening ratio r_{DB} once a bilinear shear-displacement ($V^{(DB)}$-$d^{(DB)}$) law is assumed (Figure 1c).
3. Evaluation of the equivalent viscous damping of the frame with damped braces (DBF), neglecting the hysteretic behaviour of the MIs (exactly, not considered in the case of an elastic brittle behaviour):

$$\xi_e(\%) = \xi_V + \frac{\left[\xi_F^{(h)} V_p^{(F)} + \xi_{DB} V_p^{(DB)}\right]}{\left[V_p^{(F)} + V_p^{(DB)}\right]} \qquad (1)$$

where ξ_V is a suitable value of the elastic viscous damping for the framed structure (e.g. ξ_V=5%), $\xi_F^{(h)}$ and ξ_{DB} have been calculated in steps 1 and 2, respectively, while $V_p^{(F)}$ and $V_p^{(DB)}$ represent the base-shear contributions due to the framed structure and the (hysteretic) damped braces, respectively, both at the performance point P (Figures 1b and 1c).

4. Evaluation of the effective stiffness of the equivalent damped brace ($K_e^{(DB)}$) for retrofitting a framed structure:

$$K_e^{(DB)} = K_e - K_e^{(F)};\ K_e = 4\pi^2 m_e / T_e^2 \qquad (2a,b)$$

where K_e is the effective stiffness of the damped braced frame (DBF), obtained by the effective mass m_e (=$\sum m_i\ \phi_i$) and the effective period T_e (i.e. the period corresponding to the performance displacement d_p in the displacement spectrum for ξ_e), and $K_e^{(F)}$ is the effective stiffness of the framed structure (see Figure 1b).

5. Evaluation of the strength properties of the hysteretic damped braces (HYDBs), assuming their strength distribution in such a way that they yield before the frame members yield and the infill panels reach the ultimate state. To force a simultaneous yielding of the HYDBs, the distribution law of the total horizontal component of the yielding axial forces in the HYDBs of the generic i^{th} storey ($V_{yi}^{(DB)}$) is assumed be similar to that of the analogous component of the elastic axial forces induced by the lateral loads ($V_{di}^{(DB)}$), as will be specified in the step 6 (see also Figure 1d). Therefore, the shear ratio of the HYDBs (= $V_{yi}^{(DB)}$ / $V_{di}^{(DB)}$) is assumed constant for each building storey.
6. Design of the hysteretic damped braces, aiming to obtain a damped braced structure globally regular in stiffness. More precisely, assuming a constant value of the drift ratio (Figure 1d), i.e. the ratio of the interstorey drift to the storey height (=Δ_i/h_i), the lateral stiffness of the damped braced frame at a generic i^{th} storey ($K_i^{(DBF)}$) is evaluated; then, the lateral stiffness of

the damped braces ($K_i^{(DB)}$) can be obtained once the lateral stiffness of the existing frame ($K_i^{(F)}$), consistent with the previous assumption, is calculated:

$$K_i^{(DB)} = K_i^{(DBF)} - K_i^{(F)}, \qquad i = 1, \ldots, n \tag{3}$$

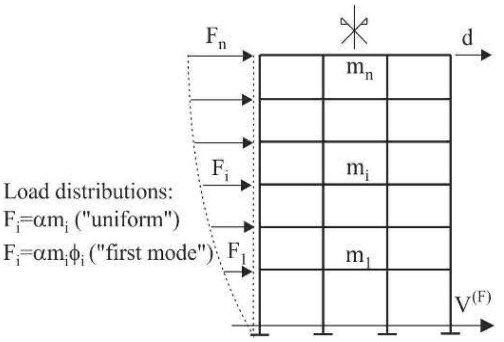

(a) Unbraced frame (F)

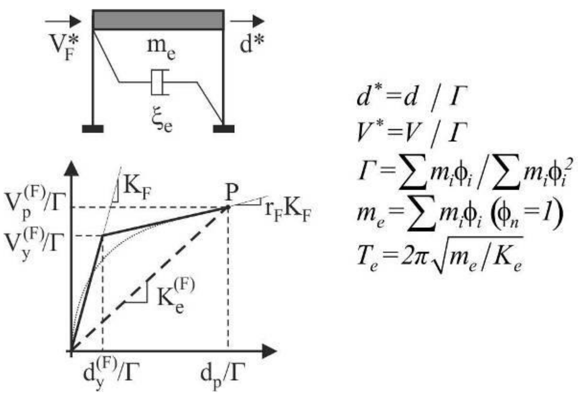

(b) ESDOF of the framed structure

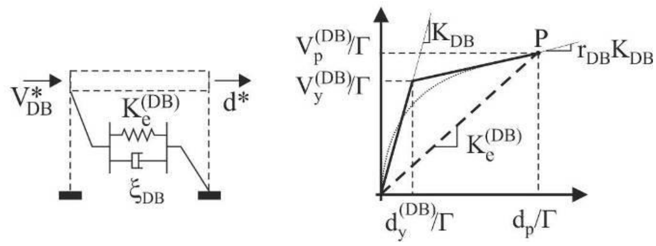

(c) ESDOF of the damped braces (DBs)

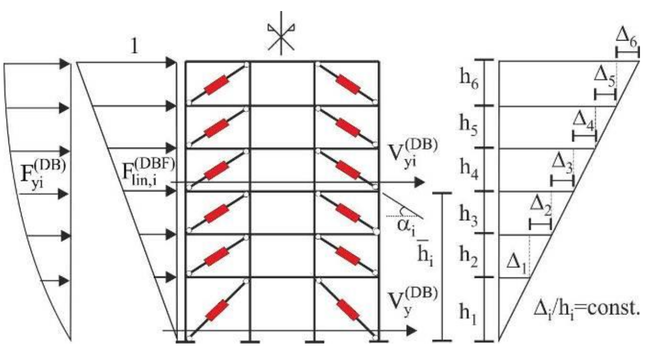

(d) HYDBs in the damped braced frame (DBF)

Figure 1 - Main assumptions for designing the hysteretic damped braces (HYDBs).

3 NONLINEAR MODELLING OF MASONRY INFILLS

In the previous works mentioned above the response of the MIs was assumed as to be simply elastic with brittle failure, neglecting in this way the hysteretic behaviour of the MIs, which can be instead important. To overcome this limitation, in this study the hysteretic behaviour of the MIs is taken into account as indicated below.

Many models with different degrees of discretization and accuracy have been proposed in the literature to reproduce the in-plane nonlinear seismic behaviour of the MIs [Liberatore *et al.*, 2017]. Each model has its advantages and limitations, but the equivalent diagonal pin-jointed strut model without tension resistance (Figure 2a) allows obtaining the key features of the inelastic response without detailed information about local phenomena. To evaluate the width (b_w) of the diagonal strut, with length d_w and total thickness t_w, the expression proposed by [Bertoldi *et al.*, 1993] is used:

$$b_w/d_w = K_1/(\lambda h) + K_2 \tag{4a}$$

$$\lambda h = \sqrt[4]{\frac{E_{w\theta}\, t_w \sin 2\theta}{4\, E_c\, I_c\, h_w}}\, h \tag{4b}$$

$$E_{w\theta} = \left[\frac{\cos^4\theta}{E_{wh}} + \frac{\sin^4\theta}{E_{wv}} + \cos^2\theta\, \sin^2\theta \left(\frac{1}{G} - \frac{2\nu}{E_{wv}}\right)\right]^{-1} \tag{4c}$$

where the dimensionless parameters K_1 and K_2 depend on the dimensionless parameter λh (see Table 1), originally proposed by [Stafford Smith, 1966], h being the centreline height of a frame storey, h_w the height of the infill panel, θ the slope of the diagonal strut with respect to the horizontal direction, E_c the elastic modulus of concrete, I_c the momentum of inertia of the columns and $E_{w\theta}$ the equivalent modulus of the infill panel expressed by Equation (4c), where E_{wh} and E_{wv} are the secant moduli of elasticity in the horizontal and vertical directions, respectively, G is the shear modulus and ν the Poisson ratio.

Table 1. Numerical values of the K_1 and K_2 parameters [Stafford Smith, 1966].

	λh<3.14	3.14<λh<7.85	λh>7.85
K_1	1.3	0.707	0.47
K_2	0.178	0.01	0.04

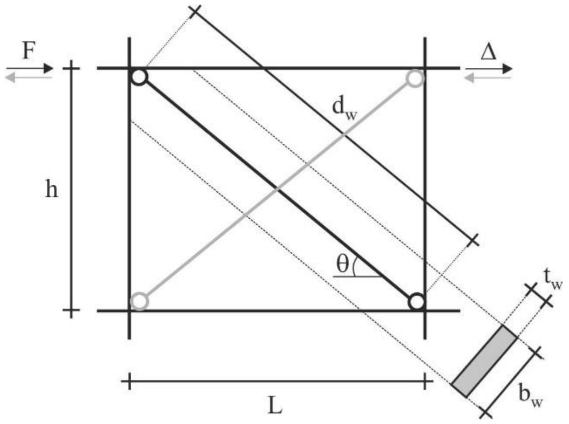

(a) Strut model

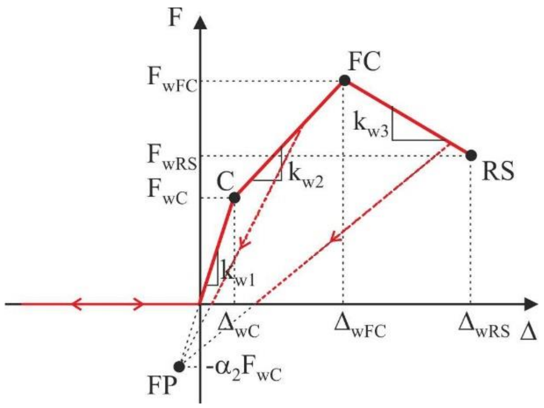

(b) Pivot hysteretic model

Figure 2. Nonlinear modelling of a masonry infill panel.

The diagonal strut model can take into account the in-plane failure modes that can occur in the infill panels when subjected to seismic loading. Four failure modes are considered, with the corresponding equivalent compressive strengths [Bertoldi *et al.*, 1993] for diagonal compression (σ_{w1}), crushing in the corners in contact with the frame (σ_{w2}), sliding shear along horizontal joints (σ_{w3}) and diagonal tension (σ_{w4}):

$$\sigma_{w1} = \frac{1.16 f_{wv} \tan\theta}{K_1 + K_2\, \lambda h} \tag{5a}$$

$$\sigma_{w2} = \frac{1.12\, f_{wv} \sin\theta \cos\theta}{K_1 (\lambda h)^{-0.12} + K_2 (\lambda h)^{0.88}} \tag{5b}$$

$$\sigma_{w3} = \frac{(1.2\sin\theta + 0.45\cos\theta) f_{wu} + 0.3\sigma_v}{b_w / d_w} \tag{5c}$$

$$\sigma_{w4} = \frac{0.6\sin\theta f_{ws} + 0.3\sigma_v}{b_w / d_w} \tag{5d}$$

where f_{wv} is the compression strength in the vertical direction, f_{wu} is the slide resistance of the mortar joints, f_{ws} is the shear resistance under diagonal compression, σ_v is the vertical compression stress due to gravity loads.

Then, the maximum lateral strength of the strut is evaluated as

$$F_w = \sigma_{w,min}\, b_w\, t_w \cos\theta \tag{6a}$$

$$\sigma_{w,min} = \min\{\sigma_{w1}, \sigma_{w2}, \sigma_{w3}, \sigma_{w4}\} \tag{6b}$$

As shown in Figure 2b, the skeleton curve of the lateral force-interstorey drift (*F-Δ*) law is described by three linear branches, which can be defined by parameters α, β and ξ [Cavaleri *et al.*, 2014]. In detail, the first ascending branch corresponds to the uncracked stage, until the attainment of point C identified by

$$F_{wC} = \alpha F_w \;, \quad \alpha = 0.4$$

$$\Delta_{wC} = F_{wC} / k_{w1} \;, \quad k_{w1} = E_{w\theta}\, b_w\, t_w \cos^2\theta / d_w$$

(7a, b, c, d)

The second ascending branch represents the post-cracking phase up to the attainment of point FC, corresponding to the full development of the cracking:

$$F_{wFC} = F_w\,; \;\; \Delta_{wFC} = \Delta_{wC} + \frac{(F_{wFC} - F_{wC})}{k_{w2}} \tag{8a,b}$$

$$k_{w2} = \beta k_{w1} \;, \quad \beta = 0.15 \tag{8c,d}$$

The third descending branch describes the post-peak strength deterioration of the infill up to the attainment of the residual values of strength and displacement (point RS):

$$F_{wRS} = 0.7 F_{wFC}\,; \quad \Delta_{wRS} = \frac{1}{\xi} \ln\left(\frac{F_{wFC}}{F_{wRS}} e^{\xi \Delta_{wFC}}\right)$$

$$\xi = 0.02\,; \quad k_{w3} = \tan\left(\frac{F_{wFC} - F_{wRS}}{\Delta_{wFC} - \Delta_{wRS}}\right)$$

(9a,b,c,d)

A pivot hysteretic model simulates the nonlinear force-displacement law of the equivalent diagonal strut (Figure 2b), based on geometrical rules that define loading and unloading branches corresponding to the unsymmetrical tension-compression behaviour of the MIs. The cyclic behaviour can be described by primary and pinching pivot points, which are governed by four parameters (α_1, α_2, β_1 and β_2) once the strength envelope, without tension resistance, is defined. However, simplifications of the pivot model can be adopted when applied to masonry infills [Cavaleri and Di Trapani, 2014]. Precisely, the hysteretic behaviour is governed by the parameter α_2(=0.25) identifying a fundamental pivot (FP) point as function of the cracking resistance (F_{wC}).

4 DESIGN OF THE HYSTERETIC DAMPED BRACES

To improve the effectiveness of the design procedure for proportioning the HYDBs in case of in-elevation irregularity of the MIs (e.g. due to soft storeys), the contribution of the MIs is taken into account considering also their nonlinear behaviour.

It should be noted that often a framed structure is designed neglecting the MIs contribution, but in reality the MIs modify the stress distribution in the frame members. Indeed, even in case of MIs regularly distributed in elevation, whose contribution can be considered comparable at each storey, the increase of stiffness and strength due to MIs, respect to the analogous properties of the bare frame, is more marked towards the upper storeys. Therefore, to compensate this increase it is reasonable inserting damped braces more stiff and strong in a lower storey rather than in an upper storey, even more in case of a soft storey.

Aiming to limit not only the plastic deformations in the frame members, but mostly to get a limited and rather uniform damage of the MIs and other nonstructural parts, it can be considered suitable assuming a same value (sufficiently limited) of the drift ratio at each storey of the infilled frame with HYDBs (i.e., Δ_i/h_i=const.; see Figure 1d). Then, with reference to two generic storeys (i, j), it can be written

$$\frac{\Delta_i}{h_i}=\frac{\Delta_j}{h_j}\ ;\ \Delta_i=\frac{V_T^{(i)}}{K_T^{(i)}}\ ;\ \Delta_j=\frac{V_T^{(j)}}{K_T^{(j)}} \tag{10a,b,c}$$

where $V_T^{(i,j)}V_T^{(i,j)}$ and $K_T^{(i,j)}$ are, respectively, the total (elastic) shear and total lateral stiffness at the two considered storeys. In particular, for a generic (i^{th}) storey, it can be written

$$V_T^{(i)}=V_F^{(i)}+V_W^{(i)}+V_{DB}^{(i)} \tag{11a}$$

$$K_T^{(i)}=K_F^{(i)}+K_W^{(i)}+K_{DB}^{(i)} \tag{11b}$$

$V_F^{(i)}$, $V_W^{(i)}$, $V_{DB}^{(i)}$ being the storey shear contributions of the bare frame, infilled walls and damped braces, respectively, while $K_F^{(i)}$, $K_W^{(i)}$, $K_{DB}^{(i)}$ are the analogous contributions to the storey (lateral) stiffness.

According to Equations (10), the total stiffness at the i^{th} storey can be expressed by the properties ($K_T^{(n)}$, $V_T^{(n)}$, h_n) of the top (n^{th}) storey:

$$K_T^{(i)}=K_T^{(n)}\frac{V_T^{(i)}}{V_T^{(n)}}\frac{h_n}{h_i} \tag{12}$$

where the total stiffness of the top storey, $K_T^{(n)}$, can be obtained, according to Equation (11b), as follows:

$$K_T^{(n)}=K_{IF}^{(n)}+K_{DB}^{(n)}=(1+\alpha_n)\,K_{IF}^{(n)} \tag{13a}$$

where

$$K_{IF}^{(n)}=K_F^{(n)}+K_W^{(n)};\quad \alpha_n=\frac{K_{DB}^{(n)}}{K_{IF}^{(n)}} \tag{13b, c}$$

$K_{IF}^{(n)}$ being the lateral stiffness of the infilled framed building at the top storey.

Then, Equations (12) and (13a) give

$$K_T^{(i)}=(1+\alpha_n)\,K_{IF}^{(n)}\frac{V_T^{(i)}}{V_T^{(n)}}\frac{h_n}{h_i} \tag{14}$$

and the lateral stiffness of the damped braces at a generic storey, $K_{DB}^{(i)}$, is obtained as

$$K_{DB}^{(i)}=K_T^{(i)}-K_{IF}^{(i)};\quad K_{IF}^{(i)}=K_F^{(i)}+K_W^{(i)} \tag{15a,b}$$

where $K_F^{(i)}$, in accordance with the initial assumption, can be calculated for the lateral loading pattern inducing the same drift ratio at each storey of the bare frame, while $K_W^{(i)}$can be assumed as the secant stiffness of the infill walls at an estimated value of the maximum drift ratio. It should be noted that a strictly necessary stiffness of the HYDB corresponds to assume α_n=0 (i.e., no damped braces at the top storey).

Finally, the yield shear contribution of all the damped braces can be obtained as

$$V_{DB,y}^{(i)}=K_{DB}^{(i)}\,\Delta_y^{(i)} \tag{16}$$

where $\Delta_y^{(i)}$ can be assumed as to be less than (or even close to) the storey drift corresponding to the first yielding of the framed part of the building under the above lateral loading pattern and/or to an acceptable state of damage of the infilled walls (or other nonstructural parts).

5 TEST STRUCTURES

5.1 *Original building*

To check the effectiveness of the design procedure proposed above, a six-storey residential building with r.c. framed structure, whose symmetric plan is shown in Figure 3a, is considered as primary test structure. This structure is designed considering the MIs as nonstructural elements regularly distributed in plan and in elevation. In Figure 3 only MIs in the corner bays of the perimeter frames are shown, supposing that the stiffness and strength contribution of the other MIs with openings (supposed rather large) is neglected. In any case the mass of all the MIs is taken into account.

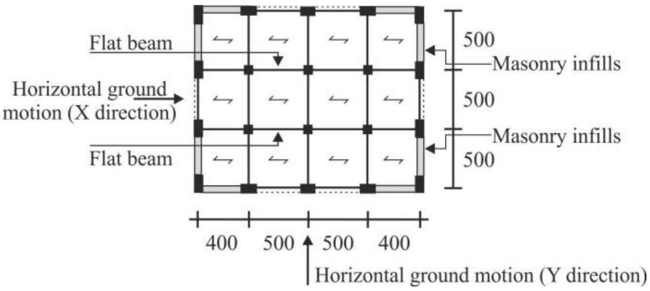

(a) Plan

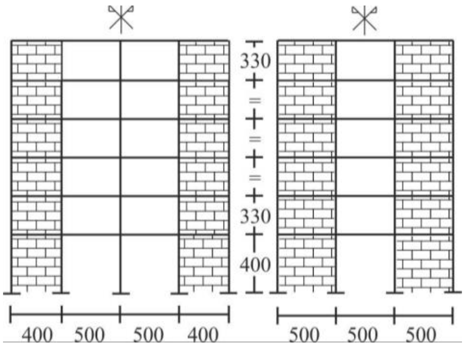

(b) Infilled perimeter frames (IF)

Figure 3. Original structure (units in cm).

The design of the original framed building is simulated in accordance with a former Italian code [DM96, 1996], assuming a medium-risk seismic region (seismic coefficient: C=0.07) and a typical subsoil class (main coefficients: R=ε=β=1). The gravity loads for the r.c. framed structure are represented by a dead load of 4.2 kN/m^2 on the top floor and 5.0 kN/m^2 on the other floors, and a live load of 2.0 kN/m^2 on all the floors; an average weight of about 2.7 kN/m^2 is considered for the masonry infill walls (two leaves).

Concrete cylindrical compressive strength of 25 N/mm^2 and steel reinforcement with yield strength of 375 N/mm^2 are considered. The cross sections of columns (i.e. corner, perimeter and central) and girders (i.e. deep and flat) are reported in Table 2. The dimensions of the r.c. members are indicated in Figure 4 for frames along the Y direction, which will be considered as that of the ground motions in the numerical investigation. Further details regarding the design of the framed structure can be found in [Mazza *et al.*, 2015] and [Mazza *et al.*, 2017].

Table 2. Cross sections of r.c. frame members (cm).

Storey	Columns			Beams	
	Corner	Perimeter	Interior	Deep	Flat
6	30x30	30x30	30x30	30x45	40x25
5	30x35	30x40	40x40	30x45	40x25
4	30x40	30x50	50x50	30x50	50x25
3	30x40	30x50	50x50	30x55	50x25
2	30x50	30x60	60x60	40x60	60x25
1	30x50	30x60	60x60	40x70	60x25

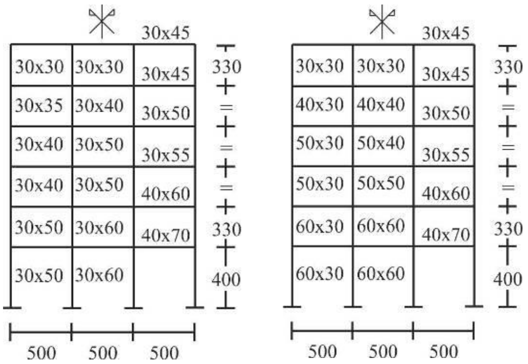

(a) Lateral frames (b) Interior and central frames

Figure 4. Dimensions of the r.c. frame members, Y direction (dimensions in cm).

Each masonry infill consists of two leaves of clay horizontal hollowed bricks, with a thickness of t_{we}=12 cm (exterior leave) and t_{wi}=8 cm (interior leave), so that the total thickness is t_w=t_{we}+t_{wi}=20 cm. The infill mechanical properties are reported in Table 3: f_{wh} and f_{wv}, compression strengths in the horizontal and vertical directions; f_{wu}, slide resistance of the mortar joints; f_{ws}, shear resistance under diagonal compression; E_{wh} and E_{wv}, secant moduli of elasticity in the horizontal and vertical directions; G, shear modulus; ν, Poisson ratio.

Table 3. Mechanical properties of the masonry infills (units in MPa; ν=0.20).

f_{wh}	f_{wv}	f_{wu}	f_{ws}	E_{wh}	E_{wv}	G
1.11	1.50	0.25	0.31	991	1873	1089

Monotonic constitutive laws of the MIs, for the six storeys of the original test structure are plotted in Figure 5 with reference to the Y direction considered in this study.

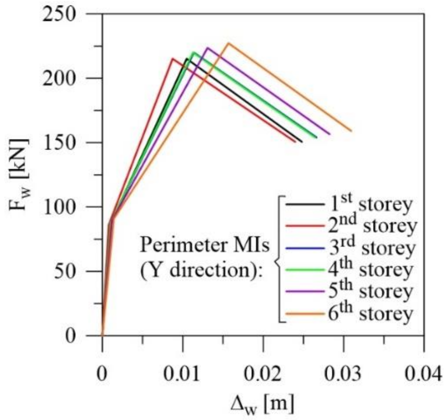

Figure 5. Monotonic curves for the masonry infills (MIs) of the original structure in the Y direction.

5.2 *Retrofitted buildings*

To simulate an irregularity in elevation, it is supposed that, due to a change in use of the building (see Figure 3), from residential to office, masonry infill walls of the first storey are removed, leading to a first soft storey framed building (IF_SS(1), Figure 6).

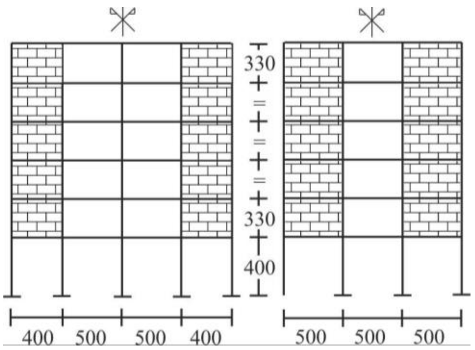

Figure 6. Soft first storey frames (IF_SS(1) building) after the change in use (dimensions in cm).

The stiffness and strength contributions of the masonry infill walls in the upper five storeys are considered idealizing any infill panel by two diagonal equivalent struts [Mainstone, 1974]. To upgrade the IF_SS(1) building from a medium- to a high-risk seismic region, diagonal steel braces with hysteretic dampers (HYDBs) are inserted at each storey. For simplicity, in Figure 7 only idealized MIs and HYDBs in the frames along the considered ground motion direction Y are shown.

The HYDBs are designed taking into account the contribution of the MIs by the procedure proposed in Section 4. As an example, two values of the parameter α_n (see Equation (13c)) are assumed, i.e. α_6=0 and α_6=1 (n=6). With reference to these two values, the total lateral (elastic) stiffnesses of the bare framed structure (K_F), infill walls (K_W, i.e. estimated secant stiffness) and hysteretic damped braces (K_{DB}), together with the total yield shear contribution of the hysteretic damped braces ($V_{DB,y}$) at each storey, are reported in Table 4 and Table 5.

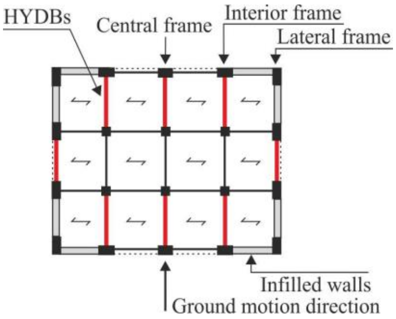

(a) Plan

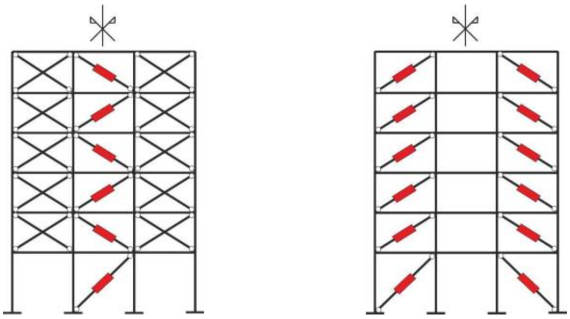

(b) Lateral frame with masonry infills and HYDBs

(c) Interior and central frames with HYDBs

Figure 7. Irregularly-infilled structure retrofitted by HYDBs (IFDB) and its modelling.

Table 4. Properties of the framed structure (F), masonry infills (W) and hysteretic damped braces (DB) - Case of α_6=0 (IFDB_K0 building).

Storey	K_F (kN/mm)	K_W (kN/mm)	K_{DB} (kN/mm)	$V_{DB,y}$ (kN)
6	74.735	83.2	0.	0.
5	120.583	83.2	151.142	748.154
4	195.291	83.2	244.172	1208.651
3	225.657	83.2	345.566	1710.554
2	405.025	83.2	266.329	1318.328
1	390.182	-----	280.472	1682.830

Table 5. Properties of the framed structure (F), masonry infills (W) and hysteretic damped braces (DB) - Case of α_6=1 (IFDB_K1 building).

Storey	K_F (kN/mm)	K_W (kN/mm)	K_{DB} (kN/mm)	$V_{DB,y}$ (kN)
6	74.735	106.6	181.335	897.608
5	120.583	106.6	587.841	2909.811
4	195.291	106.6	898.313	4446.648
3	225.657	106.6	1170.512	5794.033
2	405.025	106.6	1221.075	6044.323
1	390.182	-----	1149.856	6899.138

It should be noted that K_F has been evaluated with reference to the lateral load distribution which induces the same drift at each storey considering also axial and shear deformability of the frame members. For simplicity, an average value of the secant stiffness K_W at an expected value of the drift ratio has been assumed for the infill walls of all the upper five storeys (where MIs are still present after the change in use) and the same properties are assumed for each of the eight diagonal damped braces at a storey (i.e. $K_{DB}/8$ and $V_{DB,y}/8$, see Figure 7). The $V_{DB,y}$ value has been selected assuming for all the HYDBs a yield drift ratio of 0.15%, which is less than (but close to) the value corresponding to the first yielding of the framed structure and can be considered low enough to ensure a limited damage of the infill walls.

6 NUMERICAL RESULTS

To check the effectiveness of the design criteria illustrated above for proportioning the HYDBs in case of in-elevation irregular layout of the MIs, a numerical investigation is carried out considering also the hysteretic behaviour of the MIs. The nonlinear dynamic responses of the bare framed building (BF), infilled framed building with first soft-storey (IF_SS(1)) and infilled framed buildings with first soft-storey retrofitted by HYDBs having different properties (IFDB_K0 and IFDB_K1; see Tables 4 and 5), when subjected to a set of three artificial ground motions, are compared. Specifically, three artificial motions (duration 20 s) were generated by the code SIMQKE [Gasparini and Vanmarcke, 1976] matching the NTC18 design spetrum for the life-safety state, SLV, assuming data leading to a peak ground acceleration PGA=0.423g: i.e., a_g=0.307g (reference peak acceleration), subsoil class C, building use class III, nominal life of the building V_N=70 ys.

The nonlinear dynamic analyses are carried by SAP2000 [CSI Computers and Structures, 2017], assuming the floor slabs to be infinitely rigid on their own plane. Moreover, the r.c. frame members are idealized by a lumped plasticity model accounting for the effect of the axial load on the ultimate moment. As mentioned above, each infill wall is represented as a pair of equivalent diagonal struts connecting the frame joints (Figures 7b and 7c), whose response is simulated by the pivot hysteretic model (Figure 2b). The response of the HYDBs is simulated by a bilinear model assuming a strain hardening percentage of 1%. A viscous damping ratio of 5% associated with the first and third vibration periods is assumed. All the following results are obtained as an average of maximum values attained for the set of artificial motions.

The maximum floor displacement and the maximum inter-storey drift ratio of the four buildings considered above are compared in Figure 8a and Figure 8b, respectively. As shown in Figure 8a, the IF_SS(1) building generally exhibts the largest floor displacements, especially at the lower storeys due to the large drift at the first storey of about 1.37%, but its floor displacements become comparable to those of the BF building at the upper three storeys. However, the BF building shows the largest drift at the upper four storeys. The beneficial effect of the HYDBs is evident, especially for the IFDB_K1 building, exhibiting an almost linear curve for the maximum floor displacements and a rather uniform and low drift ratio (less than 0.34%).

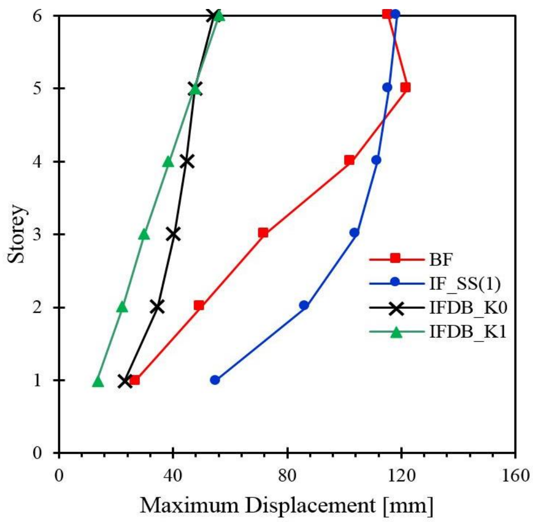

(a) Maximum floor displacements

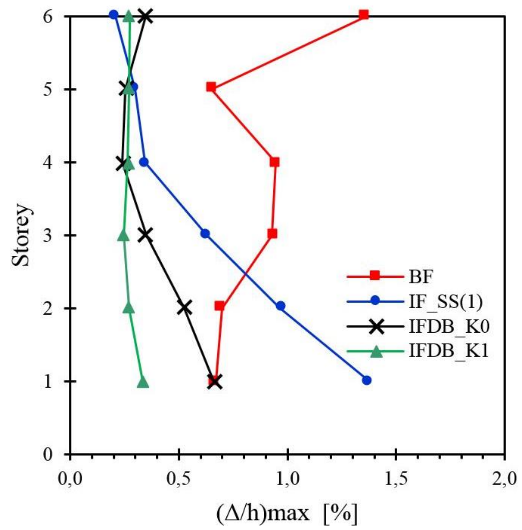

(b) Maximum inter-storey drift ratios

Figure 8. Response of the test structures.

This beneficial effect is emphasized in Figure 9, where the time history of the first and sixth storey drifts of the considered buildings subjected to one of the artificial motions are shown. In particular, both the storey drifts for IFDB_K1 building prove to be rather limited during all the time of numerical simulation.

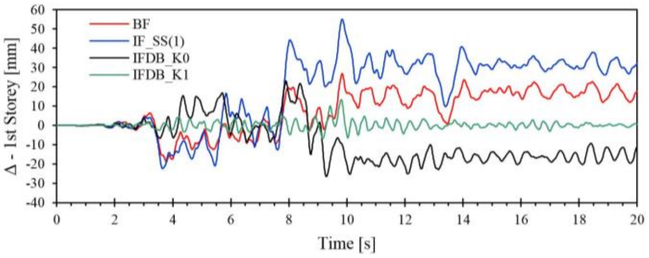

(a) At the first storey

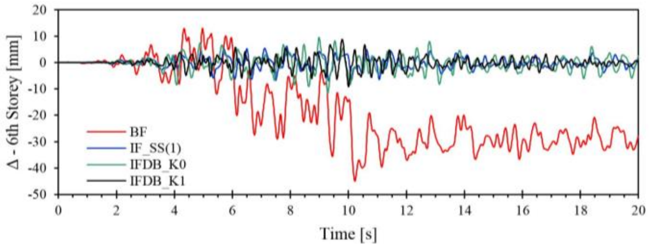

(b) At the sixth storey

Figure 9. Time-history of the drift ratio.

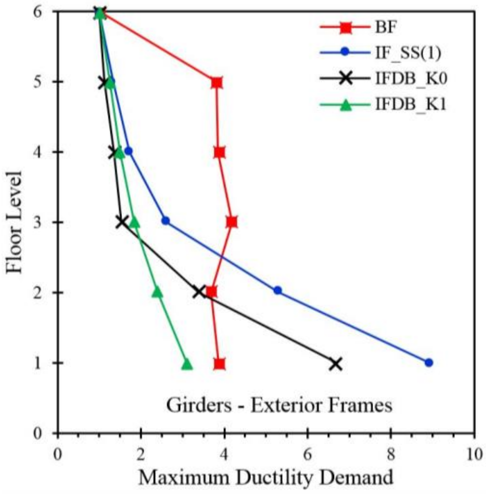

(a) Exterior frames

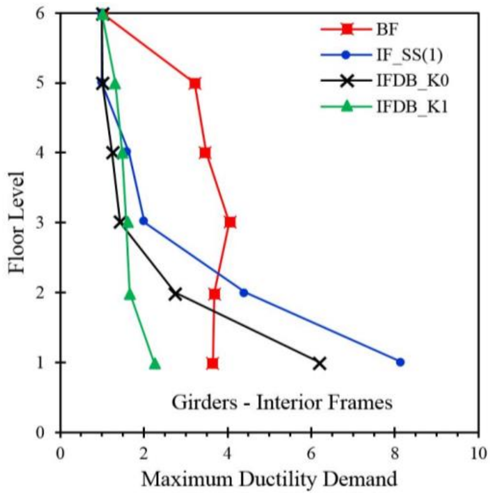

(b) Interior frames

Figure 10. Maximum ductility demand to girders.

The ductility demands to girders and columns are shown in Figure 10 and Figure 11, respectively, with reference to the exterior frames (Figures 10a and 11a) and interior frames (Figures 10b and 11b). It is interesting to observe that the ductility demands to either girders or columns exhibit a similar in-elevation distribution in both the exterior and interior frames. Moreover, for both the girders and columns the ductility demands to BF structure are larger at the upper storeys (except top-floor girders) and greater than those for the other structures, which unlike BF structure exhibit larger values at the lower storeys. The beneficial effect of the HYDBs, more marked in IFDB_K1 structure rather than in IFDB_K0 structure, is evident at the lower storeys, which undergo the detrimental effect of the first soft storey. In all the cases, the ductility demand is rather uniform and limited for IFDB_K1 structure.

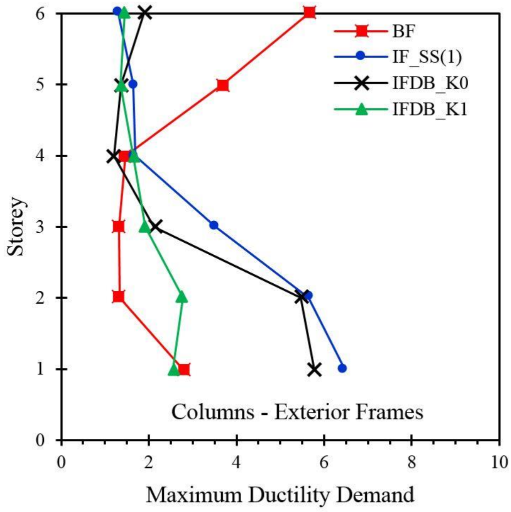

(a) Exterior frames

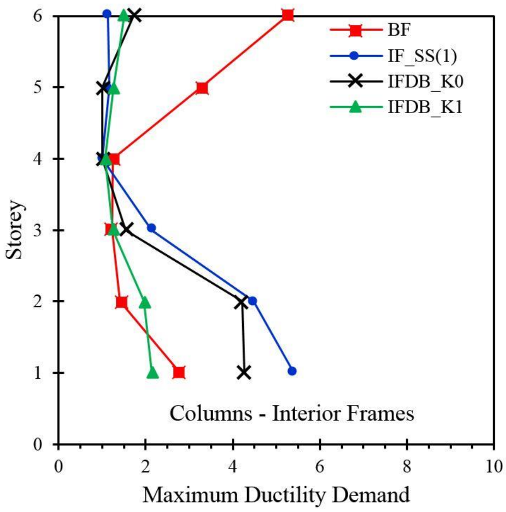

(b) Interior frames

Figure 11. Maximum ductility demand to columns.

Finally, the curves representing the ductility demand to the HYDBs at all the storeys of the retrofitted buildings are compared in Figure 12. It is evident that the ductility demand in IFDB_K1 structure is rather uniform and limited at all the storeys, exhibiting values lower than those in IFDB_K0 structure (i.e., that without HYDBs at the top storey). A more limited plastic excursion of the HYDBs of IFDB_K1 structure, in comparison with the HYDBs of IFDB_K0 structure, was pointed out also in a previous work by the authors (Mazza *et al.*, 2018), comparing the hysteretic responses of the HYDBs at each storey. As an example, in Figure 13 it shown the hysteretic response of HYDBs at first storey of the IFDB_K0 building.

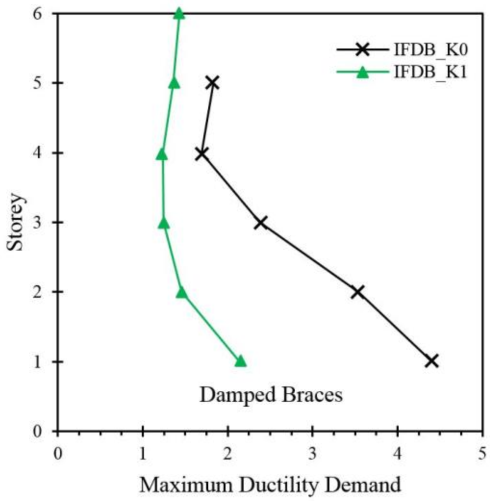

Figure 12. Ductility demand to HYDBs of the retrofitted buildings.

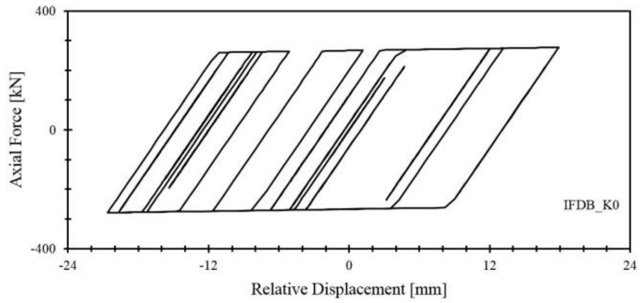

Figure 13. Hysteretic response of HYDBs at the first storey of IFDB_K0 building.

7 CONCLUSIONS

Design criteria to proportion HYDBs for the sesmic retrofitting of r.c. framed buildings with in-elevation irregular layout of the masonry infills have been proposed aiming to obtain the same drift ratio at each storey. To check the effectiveness of the proposed design criteria in the case study of a r.c. six-storey building, the nonlinear seismic responses of the bare framed building (BF), first soft-storey building (IF_SS(1)) and first soft-storey building retrofitted by HYDBs having different properties (IFDB_K0 and IFDB_K1), all subjected to a set of artificially generated motions, are compared. Specifically, two different stiffness levels of the HYDBs have been assumed: i.e. α_6=0 (IFDB_K0, without HYDBs at the top storey) and α_6=1 (IFDB_K1, having HYDBs with the same lateral stiffness of the infilled frame at the top-storey).

The results have shown that the selection of HYDBs having strictly necessary stiffness (i.e. α_6=0) allows to control the response of the soft-storey building reducing floor displacements, drifts and ductility demand to the r.c. frame members. On the other hand, to limit considerably these response parameters and get a rather uniform in-elevation distribution of the drift ratio and ductility demand to r.c. members and HYDBs, it is necessary adopting rather rigid and strong HYDBs (e.g., assuming α_6=1), but this can lead to a high variation of the axial forces in the columns. In such a case it can be advisable to distribute in many frames the total stiffness and strength required to the HYDBs.

Even though the present study clarified important aspects in proportioning the HYDBs, further information can be obtained extending the parametric study to different cases of irregularly infilled buildings subjected to real ground motions with intensity corresponding to different performance levels.

ACKNOWLEDGEMENTS

This work was financed by Re.L.U.I.S. (Italian network of university laboratories of earthquake engineering), within the “Convenzione D.P.C.–Re.L.U.I.S. 2019-21, Progetto WP15, Contributi normativi per Isolamento e Dissipazione”.

REFERENCES

Bertoldi, S.H., Decanini, L.D., Gavarini, C. (1993). Telai tamponati soggetti ad azione sismica, un modello semplificato: confronto sperimentale e numerico. *6° Convegno Nazionale di Ingegneria Sismica, ANIDIS*, Perugia, Italy, 815-824 (in Italian).

Braga, F., Manfredi, V., Masi, A., Salvatori, A., Vona, M. (2011). Performance of non-structural elements in RC buildings during the L’Aquila, 2009 earthquake. *Bulletin of Earthquake Engineering*, **9**(1):307-324.

Cavaleri, L. and Di Trapani, F. (2014). Cyclic response of masonry infilled RC frames: experimental results and simplified modelling. *Soil Dynamics and Earthquake*

Engineering, **65**:224-242.

Cavaleri, L., Papia, M., Macaluso, G., Di Trapani, F., Colajanni, P. (2014). Definition of diagonal Poisson's ratio and elastic modulus for infill masonry walls. *Materials and Structures*, **47**:239-262.

CSI Computers and Structures (2017). *SAP2000 v19 Integrated Finite Element Analysis and Design of Structures*.

DM96 (1996). *Norme tecniche per le costruzioni in zone sismiche*, Ministro dei Lavori Pubblici, D.M. 16-01-1996, G.U. 5-2-1996; Circolare 10-04-1997 N. 65/AA.GG, G.U. n. 97, 28-4-1997 (in Italian).

Eurocode 8 (2003). *Design of structures for earthquake resistance - part 1: general rules, seismic actions and rules for buildings*. C.E.N., European Committee for Standardization.

Federal Emergency Management Agency, *FEMA 356 (2000): Prestandard and commentary for the seismic rehabilitation of buildings*. American Society of Civil Engineers, Reston, Virginia.

Gasparini, D. and Vanmarcke, E. (1976). *Simulated earthquake motions compatible with prescribed response spectra*. Massachusetts Institute of Technology, Department of Civil Engineering, U.S.A..

Hak, S., Morandi, P., Magenes, G., Sullivan, T.J. (2012). Damage control for clay masonry infills in the design of rc frame structures. *Journal of Earthquake Engineering*, **16**(S1):1-35.

Liberatore, L., Noto, F., Mollaioli, F., Franchin, P. (2017). A comparative assessment of strut models for the modelling of in-plane seismic response of infill walls. COMPDYN 2017, *6th ECCOMAS Thematic Conference on Computational Methods in Structural Dynamics and Earthquake Engineering*, Rhodes, Greece, 2:3255-3268.

Mainstone, R.J. (1974). *Supplementary note on the stiffness and strength of infilled frames*. Current Paper CP13/74, Building Research Establishment, London.

Mazza, F. and Vulcano, A. (2014). Design of hysteretic damped braces to improve the seismic performance of steel and r.c. framed structures. *Ingegneria Sismica*, **1**:5-16.

Mazza, F., Mazza, M., Vulcano, A. (2015). Displacement-based seismic design of hysteretic damped braces for retrofitting in-elevation irregular r.c. framed structures. *Soil Dynamics and Earthquake Engineering*, **69**:115-124.

Mazza, F., Mazza, M., Vulcano, A. (2017). Nonlinear seismic response of irregularly masonry-infilled r.c. framed buildings retrofitted with hysteretic damped braces. *Proceedings 16th World Conference on Earthquake Engineering*, Paper No. 476, Santiago, Chile.

Mazza, F., Mazza, M., Vulcano, A. (2018). Seismic retrofitting of in-elevation irregularly infilled r.c. framed structures by hysteretic damped braces. *Proceedings 16th European Conference on Earthquake Engineering*, Paper No. 11533, Thessaloniki, Greece.

NTC18 (2018). *Aggiornamento delle "Norme tecniche per le costruzioni"*, Ministero delle Infrastrutture dei Trasporti, D.M. 17-01-2018, G.U. 20-2-2018; Circolare 21-01-2019, n. 7 C.S.LL.PP, G.U. 11-2-2019 (in Italian).

Priestley, M.J.N., Calvi, G.M., Kowalsky, M.J. (2007). *Displacement-based seismic design of structures*. IUSS Press, Istituto Universitario di Studi Superiori di Pavia, Italy, Vol. 1, Redwood City, CA.

Soong, T.T. and Dargush, G.F. (1997). *Passive Energy Dissipation Systems in Structural Engineering*. John Wiley & Sons Ltd, Chichester, England.

Stafford Smith, B. (1966). Behaviour of square infilled frames, *Journal of the Structural Division*, **92**(1):381-403.